Interfacial fracture parameters & size effect in concrete-concrete cold joints

P. Subba Rao & J. M. Chandra Kishen
Department of Civil Engineering

Indian Institute of Science

Bangalore 560 012, India

ABSTRACT: The behavior of concrete-concrete, transverse cold jointed interface beams is experimentally investigated in order to determine the fracture energy. Simply supported beams under three-point bending with different compressive strengths of concrete on either side of the interface are considered. It is found that the fracture energy decreases as the difference between the compressive strength of the material on either side of the interface increases. Further, the size of the process zone is found to remain constant for all combination of interfaces considered. In addition, three different sizes of geometrically similar interface specimens are considered to study the size effect using Bazant's size effect model proposed for concrete specimens. It is found that interface specimens exhibit size effect similar to intact concrete specimens and the slope of the nominal strength versus size on a log-log plot is –1/2, indicating the applicability of linear elastic fracture mechanics for large specimens.

Keywords: cold jointed interface, fracture energy, size effect.

1. INTRODUCTION

Repair and rehabilitation of concrete structures is a common requirement in modern construction. This can be successful if the new material interacts effectively with the parent concrete. Compatibility between repair material & substrate concrete is important for prevention of cracking but reliable quantification of the required parameters is lacking [Mangat and Flaherty (2000)]. Restrained contraction of repair materials with the restraint being provided through the bond to the existing concrete substrate, significantly increases the complexity of repair projects compared to new construction. Volume changes are the causes of contraction that often result in cracking and debonding of the repaired section. The weak transition zone between new and old concrete controls many properties of repaired concrete. It has been shown [Li et al (2001)] that the interface between new & old concrete is the weakest link in repaired concrete. Reinhardt (1982) tested specimens consisting of two pieces of pre-fabricated concrete adhered together using mortars of different compressive strengths. He treated the joint as a discontinuity and its strength was assumed to be due to cohesion between the joined parts. He reported that specimens adhered by mortars with higher compressive strengths followed LEFM solutions. Buyukozturk et al (1992) have studied fracture of interfaces between dissimilar materials and found that the experimental results were in agreement with LEFM on the aggregate mortar sandwich specimens. Wang and Maji (1993) conducted uniaxial tension tests on mortar-limestone interface specimens to obtain the bridging stress versus crack opening displacement curve. They reported that both mechanical interlock and chemical interaction contribute to the interface bonding between mortar

and limestone whereas only mechanical interlocking is likely responsible for the bond between mortar and rock salt. Chandra Kishen (1996) conducted tests on limestone-concrete interface compact tension specimens to obtain the fracture parameters. The author reported that the difference in the behavior between intact and interface specimens lies in their post-peak load deformation behavior.

In most of the work reported, the interface between different materials is considered. However, there is very little information about the cracking and fracture process at the interfaces between new & old concrete. This information is required to study the cracking behavior of patch-repaired systems that are commonly encountered in the rehabilitation of damaged concrete structures. Furthermore, in large concrete structures such as dams, cold joints between successive lifts are inevitable. Therefore, in this paper, fracture parameters of the interface between different concrete mixes are obtained by conducting tests on beams with concrete-to-concrete cold joints. In addition, beams of different depths are used, in order to study the size effect on the failure stress.

2. EXPERIMENTAL PROGRAMME.

In the present work, beams having a transverse cold joint between two different strengths of concrete are tested under three point bending. Geometrically similar notched beams of three different depths, with span to depth ratio of 2.5, notch to depth ratio of 0.1 and notch width of 2 mm are used. Figure 1 shows the geometry of the beam. The cross-sectional dimensions and span of the beams are shown in Table-1. The thickness of all the beams is kept constant at 50 mm.

Four different concrete mixes A, B, C and D with compressive strengths as shown in Table-2 are used for preparing the beams. The different
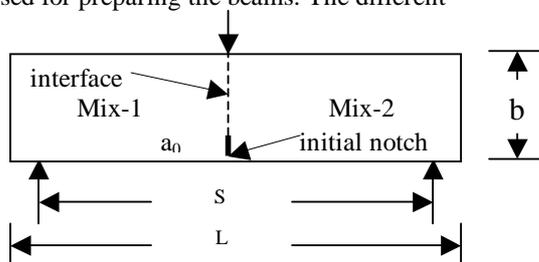
Figure 1 Notched beam (with interface)

combinations of material/concrete mix on either side of the interface used for preparing the specimens are shown in Table 3 along with their designation.

Table 1. Sizes of beams used in the tests

S .No	Beam	b	s	L
		mm	mm	mm
1	Small	76	190	241
2	Medium	152	380	431
3	Big	304	760	810

The specimens are prepared by casting the first half of beam with concrete of mix A (Table 2). The second half of the beam with concrete mixes A, B, C and D (Table 2) are cast after two days. This creates a cold joint between the two mixes of concrete. A notch is introduced at the interface during the casting process itself. An intact beam (without an interface) with concrete mix A is also prepared. The specimens are demoulded after two days of casting the second mix and placed in water for curing.

Table 2. Compressive strength of different mixes

S. No	Mix	Compressive strength N/mm^2
1	A	28
2	B	39
3	C	51
4	D	58

Table 3: Designation of beams

Specimen Designation	Remarks
A	No interface. Intact beam of mix A
AA	Cold joint between mixes A & A
AB	Cold joint between mixes A & B
AC	Cold joint between mixes A & C
AD	Cold joint between mixes A & D

The beams were tested in a closed-loop servo-hydraulic testing machine under CMOD control. The CMOD was monitored using a clip gage. Typical load – CMOD plots obtained for interface

small beam AD and intact small beam A are shown in Figures 2 and 3 respectively. The average peak loads of the beams for various interfaces and that of intact beams are shown in Table 4. It is seen that the maximum load carrying capacity of interface beams decreases when the difference in the strengths on either side of the interface increases. Further, as the size of the specimen increases the maximum load carrying capacity also increases.
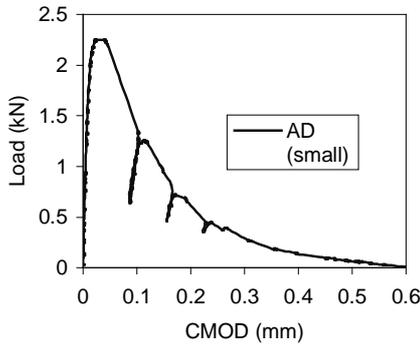
Figure 2 Load-CMOD plot of interface notched small beam AD
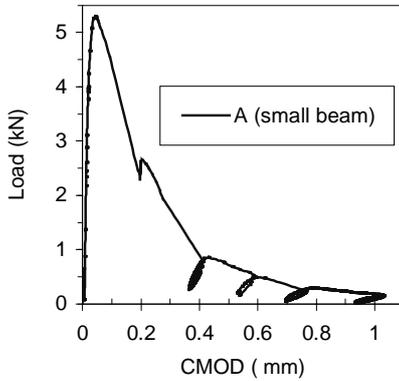
Figure 3 Load-CMOD plot of intact small notched beam A

Table 4. Average peak load, P^0_j (kN)

S.No	Beam	A	AA	AB	AC	AD
1	Small	5.5	3.7	3.1	2.8	2.4
2	Medium	8.1	5.4	4.6	4.1	3.6
3	Big	11.4	7.6	6.4	5.9	5.1

3. DETERMINATION OF FRACTURE ENERGY

The fracture energy of interface specimens is determined using the RILEM (1999) methods which is based on the size effect model by Bazant et al (1987,1990) for concrete. In this method only the maximum loads P_1, P_2, ……. P_n, for specimens for various sizes b_1, b_2 …….. b_n and the modulus of elasticity E are needed to determined the values of fracture energy G_f [Shah et al (1995)] The corrected maximum loads P_1^0 , P_2^0 and P_3^0 which takes the weight of the specimen in to account, are calculated using

$$P_j^0 = P_j + \frac{2S_j - L_j}{2S_j} gm_j \qquad (1)$$

where (j =1,2,3), m_j is mass of the specimen j, g = 9.81 m/s^2, S_j and L_j are as shown in Figure 1. By introducing

$$Y_j = \left[\frac{b_j t}{P_j^0}\right]^2 \ and \ X_j = b_j \qquad (2)$$

for j = 1,2, & 3, a linear regression

$$Y = A_B X + C_B \qquad (3)$$

is plotted as shown in Figure 4. where A_B is the value of slope & C_B the intercept on the Y-axis. Since the specimens used in the tests had a ratio of S/b = 2.5, a geometric factor $g(\alpha_0)$ is calculated with $\alpha_0 = a_0/b$ using [Shah et al (1995)],

$$g(\alpha_0) = \left(\frac{S}{b}\right)^2 \pi\alpha_0 [1.5 g_1(\alpha_0)]^2 \qquad (4)$$

$$g_1(\alpha_0) = \frac{1 - 2.5\alpha_0 + 4.49\alpha_0^2 - 3.98\alpha_0^3 + 1.33\alpha_0^4}{(1-\alpha_0)^{3/2}}$$

(5)

The fracture energy is determined using

$$G_f = \frac{g(\alpha_0)}{EA_B}$$

(6)

The length of the fracture process zone for an infinitely large specimen c_f is obtained using

$$c_f = \frac{g(\alpha_0)}{g'(\alpha_0)}\left[\frac{C_B}{A_B}\right]$$

(7)

where $g'(\alpha_o)$ is the first derivative of $g(\alpha_o)$.

The modulus of elasticity of the interface specimens are obtained from a typical load-CMOD curve shown in Figures 2 & 3 using the relationship

$$E = \frac{6Sa_0 g_2(\alpha_0)}{C_i b^2 t}$$

(8)

where C_i is the initial compliance and $g_2(\alpha_0)$ is geometric factor calculated from

$$g_2(\alpha_0) = 0.76 - 2.28\alpha_0 + 3.87\alpha_0^2 - 2.04\alpha_0^3$$
$$+ \frac{0.66}{(1-\alpha_0)^2}$$

(9)

Equivalent young's moduli of various interfaces and material properties of the interfaces namely fracture energy (G_f) and size of process zone (c_f) computed as detailed above are shown in Table 5. It is seen that the fracture energy decreases as the difference in specimen strength between the mixes on either side of the interface increases. This implies that greater the difference in compressive strength between the parent and repair material in patch repair systems, greater is the vulnerability to cracking for the same loading system. Further, it is seen that the size of the process zone remains constant for all the mix ratio combinations considered. It may be noted that there is no aggregate interlock mechanism in the case of interface as observed in intact specimens. Hence, the process zone, which is formed due to the
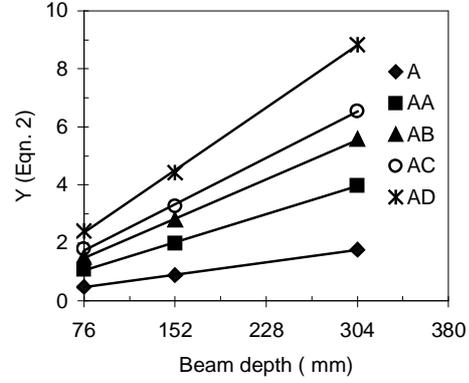
Figure 4: Linear regression plot

cohesive forces only, remains constant for interface between different mixes of concrete.

Table 5. Material properties.

Specimen	E GPa	G_f N/m	C_f mm
A	20.91	31.82	0.70
AA	12.91	23.13	0.61
AB	10.65	19.89	0.66
AC	9.76	18.50	0.66
AD	7.54	17.77	0.66

4. SIZE EFFECT IN FRACTURE AT INTERFACE.

The size effect is the most compelling reason for adopting fracture mechanics in design. It is known that in the conventional plastic limit analysis, the load capacity or the fracture criterion expressed in terms of stress remain constant for any size of structure and for any given geometry. By contrast, failures governed by linear elastic fracture mechanics exhibit a rather strong size effect. For concrete structures, the curve obtained by plotting strength versus size on log-log plot approaches a horizontal line for the strength criterion if the structure is very small and an inclined straight line of slope –1/2 if the structure is very large [Bazant and Planas (1997)].

In this work, interface specimens of three different sizes are considered for verifying whether size

effect is seen to be similar to that observed in intact concrete structures. Bazant's size effect law proposed for concrete structures is used in this study for interfaces. Figure 5 shows a plot of nominal strength versus the size (depth) of the interface specimen on log-log scale.
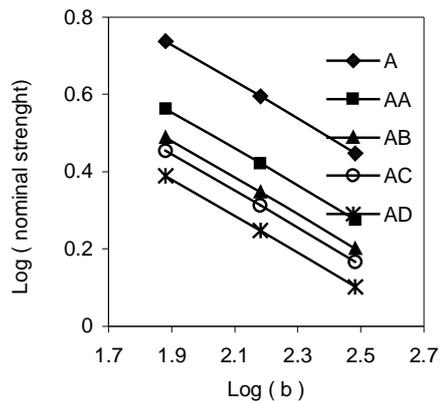
Figure 5. Size effect plot for interface specimens.

In this figure, the nominal strength is computed using

$$\sigma_{NC} = \left[C_n^2 EG_f / \{ g'(\alpha_o)C_f + g(\alpha_o)D \} \right]^{1/2}$$

(10)

where D is depth of the specimen, E is the equivalent elastic modulus of the interface (Table 5), G_f the fracture energy (Table 5), $g'(\alpha_0)$, C_f and $g(\alpha_0)$ are as explained earlier. C_n is test specimen constant which is equal to 1.5 times span to depth ration of the geometrically similar beam specimens. In this figure, it is seen that the slope of the inclined straight lines are almost equal to – 1/2 as seen even for intact concrete specimens. This implies that the failure of large interface specimens is also governed by linear elastic fracture mechanics.

5. CONCLUSIONS

In this work, beams having cold jointed interface between concrete-concrete with different mixes on either side are subjected to three-point bending test in order to obtain the fracture parameters such as the fracture energy and the size of the process zone. Further, the size effect in these specimens is studied by testing geometrically similar specimens of three different sizes. The following conclusions are made from this study:

1. The fracture energy of interface decreases as the difference in the compressive strengths of the material on either side of the interface increases. This implies that the compressive strength of a patch-repaired concrete should not be very much different from that of the parent concrete in patch repair systems.

2. The size of the process zone formed near an interface crack is found to be constant for all combination of concrete mixes on either side of the interface. This implies that the process zone size depends strongly on the aggregate interlock mechanism as observed in the case of intact concrete specimens. This mechanism is absent for interface specimens.

3. In the case of interface specimens, size effect very similar to that in intact specimen is observed indicating that the failure stress is governed by fracture mechanics concepts for large specimens.

6. REFERENCES

Bazant, Z.P. and Pfielfer, P.A. 1987. *Determination of fracture energy from size effect and brittleness number*. ACI Materials Journals. Vol. 84, No.6. pp-463-480.

Bazant, Z.P. and Kazemi, M.T. 1990. *Determination of fracture energy, process zone length and brittleness number*. International Journal of Fracture, Vol. 44, pp-111-131.

Bazant, Z.P. and Planas, J. 1997. *Fracture and size effect in concrete and other quasibrittle materials*. CRC press, USA.

Buyukozturk, O. and Lee, K.M. 1992. *Interface fracture mechanics of concrete composites*. Proceedings of FraMCoS 1,edited by Bazant, Z.P. Elsevier Applied Science, London, pp. 163-168.

Chandra Kishen, J. M. 1996. *Interface cracks: fracture mechanics studies leading towards safety assessment of dams*. PhD thesis, Dept. of civil, environmental and architectural engineering, University of Colorado, Boulder, USA.

Lee, K.M., Buyukozturk, O. and Oumera, A. 1992. *Fracture analysis of mortar-aggregate interfaces in concrete*. Journal of Engineering Mechanics , Vol. 118, No. 10 , pp-2031-2047.

Li, G., Xie, H. and Xiong, G. 2001. *Transition zone studies of new-to-old concrete with different binders*. Cement and Concrete Composites.23, pp. 381-387.

Mangat, P.S. and Flaherty, F.J. 2000. *Influence of elastic modulus on stress redistribution and cracking in repair patches.* Cement and Concrete Research,. 30, pp. 125-136.

Reinhardt, H.W. 1982. *Length influence on bond strength in composites precast concrete slabs.* International Journal of Cement Composites and Light weight Concrete, Vol. 4, No. 3 pp-139-143.

RILEM Committee on Fracture Mechanics of Concrete-Test Methods, 1990. S*ize effect Method for determining fracture energy and process zone size of concrete*, Materials and Structures, vol.23, pp-461-465.

RILEM Committee on Fracture Mechanics of concrete-Test Methods, 1990. Determination of the fracture parameters (K^s_{1C} and $CTOD_C$) of plain concrete using three-point bend tests. Materials and Structures, Vol. 23, pp. 457-460.

Shah, S.P., Swartz, S.E. and Ouyang, C. 1995. *Fracture mechanics of concrete: Applications of fracture mechanics to concrete, rock and other quasi-brittle materials.* Wiley-Interscience Publications.

Wang, J. and Maji, A.K. 1993. Experimental studies and modeling of the concrete/rock interface. ACI Spring Convention, Vancouver.

.